Energy &
Environmental Science

Cite this: *Energy Environ. Sci.*, 2012, **5**, 6763

www.rsc.org/ees

PERSPECTIVE

Recent progress in electrochemical hydrogen production with earth-abundant metal complexes as catalysts

Mei Wang,[*a] **Lin Chen**[a] **and Licheng Sun**[*ab]

Received 28th November 2011, Accepted 17th February 2012
DOI: 10.1039/c2ee03309g

This perspective article reviews the recent important progress in electrocatalytic hydrogen production catalyzed by earth-abundant metal complexes. The catalysts are divided into two categories depending on the media used in the hydrogen-evolving reactions, with an emphasis on the types of acids employed. The catalysts used in the first category, which work in organic solutions, include nickel and cobalt complexes with base-containing diphosphine ligands, cobaloximes, cobalt tetrapyridine complexes, and [NiFe]- and [FeFe]-hydrogenase mimics. Molybdenum and cobalt pentapyridine complexes, as well as the cobalt bis(iminopyridine) complex reported very recently, are the most important examples of catalysts used in the second category, which work in aqueous solutions. The advantages and disadvantages of the different types of catalysts are discussed and the hydrogen-evolving mechanisms for the well-studied catalysts are illustrated. In addition, several molecular catalyst-modified electrodes for hydrogen production are described.

1 Introduction

Global energy concerns due to the limited reserves of fossil fuels and the CO_2 over-discharge problem, accompanied by the burning of fossil fuels, have signalled the urgent need to find clean, safe and sustainable alternatives to fossil fuels.[1–5] Hydrogen is an ideal energy carrier with an energy density of 140 MJ kg^{-1} and water as its combustion product. Besides the technical barriers for storage, transportation and utilization of H_2, the development of energy-efficient, cost-effective and clean processes for H_2 production is one of the greatest challenges to successfully shift from a fossil fuel-based economy to a hydrogen economy. Water is the most promising source for the production of H_2 as it is carbon-free, plentiful and almost costless. A highly desirable strategy is photoinduced water splitting into hydrogen and oxygen using sunlight as the sole energy source, to build a clean and sustainable energy cycle. Basically, the water splitting reaction can be divided into two half reactions: water oxidation and water reduction. Although the ultimate goal is to couple catalyst systems for the two halves of the reaction to an integrated efficient device for whole water splitting, one of the crucial issues that must be solved in advance is the development of highly efficient and durable catalyst systems for water oxidation and reduction.

The development of electrocatalysts for water (proton) reduction to H_2 is meaningful and important for the final purpose of light-driven H_2 production, taking the following aspects into consideration: 1) photoelectrochemical devices can

Broader context

The development of earth-abundant metal-based catalysts with high efficiencies, low overpotentials and long durability for electrocatalytic H_2 production is part of the important work for finally constructing whole water-splitting photoelectrochemical cells. Although encouraging progress has been achieved in discovering new proton reduction catalysts and understanding the mechanisms of catalytic H_2-evolving reactions, only a molybdenum and two cobalt complexes have been reported as being active for electrochemical H_2 production with moderate to large overpotentials in neutral aqueous solutions. All other earth-abundant metal-based molecular catalysts reported in recent years function in organic media with different acids as proton sources. Highly active, energy efficient, robust and inexpensive water reduction catalysts are urgently required for electrochemical H_2 production without the need of extra acids and organic solvents.

---

[a] *State Key Laboratory of Fine Chemicals, DUT–KTH Joint Education and Research Center on Molecular Devices, Dalian University of Technology (DUT), Dalian 116024, China. E-mail: symbueno@dlut.edu.cn*
[b] *Department of Chemistry, School of Chemical Science and Engineering, KTH Royal Institute of Technology, 10044 Stockholm, Sweden. E-mail: lichengs@kth.se*

be designed either with both half reactions driven by light or only water oxidation driven by light. In the latter case, which is accompanied by the evolution of O_2 from the side of the device where water oxidation takes place, electrons and protons are provided to the water reduction side of the device and the protons are catalytically reduced to H_2 by a water reduction catalyst in the dark; 2) hydrogen production by the electrolysis of water with a low overpotential and high efficiency could be a convenient way to store energy if the electric power is obtained from renewable sources of electricity, such as solar cells; 3) electrochemical proton reduction to H_2 is a simple and convenient means to test the efficiency of newly synthesized catalysts and to estimate the reduction potentials required for the realization of the desired photoinduced electron transfer processes, as well as the investigation of the mechanisms of H_2 formation. This perspective article will focus on the electrochemical production of H_2 from the reduction of water or acids using earth-abundant metal complexes as the catalysts, which have been reported over the last decade.

Currently, only platinum and its alloys are used as highly efficient and durable catalysts for electrochemical H_2 production. Almost all other electrode materials and electrocatalysts now available display a kinetic limitation for the electrochemical proton reduction to H_2. Platinum metal is an excellent catalyst for water splitting and H_2 production; however, it is not a sustainable material for large-scale applications due to its limited reserves on Earth. The progress in the study of hydrogenases have injected new vitality into the investigation of homogeneous catalyst systems for H_2 production from water. Studies on earth-abundant metal molecular catalysts for electrochemical H_2 production over the last decade have mainly concentrated on [FeFe]- and [NiFe]-dinuclear complexes, which mimic the hydrogenase active sites, cobaloxime complexes, nickel and cobalt complexes with base-containing diphosphines, and cobalt and molybdenum complexes with polypyridine ligands. Several reviews have summarized the advances in the fields of iron-,[6–8] cobalt-[9,10] and nickel-based[11–13] electrocatalysts, with an emphasis on the structures of the catalysts and the mechanisms of the catalytic reactions. Considering their future practical applications, in addition to the catalytic activity, overpotential and durability, the working medium and the proton source required by a H_2-evolving catalyst system are two important factors for evaluating a homogeneous electrocatalyst. In this perspective, we will review the recently reported efficient homogeneous electrocatalysts composed of iron, cobalt, nickel and some other abundant metals, and the sections are divided depending on the working media and proton sources of the catalyst systems. A brief description on the principles and methods for evaluating the electrochemical H_2-production molecular catalysts will be introduced in the following section, because different methods have been used in the literature to assess the efficiencies of various electrocatalysts. In the third and forth sections, homogeneous electrochemical H_2-evolving systems using earth-abundant metal complexes as molecular catalysts *in organic solvents and aqueous solutions* will be dealt with separately. Electrochemical devices incorporating earth-abundant metal complexes for the production of H_2 from the reduction of water or acids are described in the fifth section. The problems that exist in current electrochemical H_2-production systems are discussed and future challenges and developments are envisaged in the final section.

Mei Wang

Prof. Mei Wang received her PhD in 1989 from Dalian Institute of Chemical Physics (China). Afterwards she worked as an Alexander von Humboldt fellow from 1989 to 1991 at Technische Universität München. She has been a full professor at Dalian University of Technology (China) since 2002. Her research interests are focused on chemical mimics of hydrogenases, photoinduced water splitting and hydrogen production with non-precious metal-based catalysts.

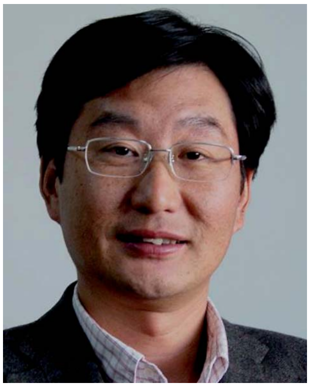

Licheng Sun

Prof. Licheng Sun received PhD in 1990 from Dalian University of Technology. He worked as a postdoc at Max-Planck-Institut für Strahlenchemie with Dr Helmut Görner (1992–1993) and Freie Universität Berlin (1993–1995) as an Alexander von Humboldt fellow with Prof. Dr Harry Kurreck. He became an assistant professor in 1997 at KTH Royal Institute of Technology and in 1999 at Stockholm University, and a full professor in 2004 (KTH). He has published more than 280 peer reviewed articles in the fields of molecular solar cells and solar fuels and has a h-index of 43.

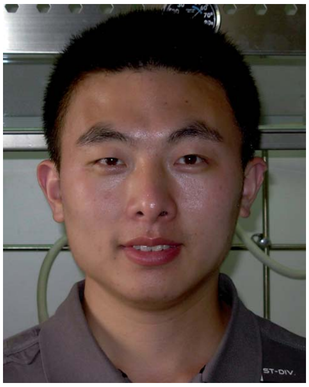

Lin Chen

Lin Chen studied chemistry at the Dalian University of Technology and received his BS in 2007. Now he is working for his PhD thesis, which is focused on the synthesis and electrochemistry of bio-inspired diiron complexes related to the active site of FeFe-hydrogenases, with emphasis on the design and synthesis of efficient H_2-evolving catalysts based on non-precious metals.

2 General principles and methods for the evaluation of homogeneous molecular electrocatalysts for H_2 production

As studies on electrochemical H_2 production were made in different media using various acids with different working and reference electrodes, it is impossible to evaluate the efficiencies of electrocatalysts by directly comparing the turnover frequencies (TOF) and catalytic potentials observed by different research groups. The working electrodes commonly used in electrochemical H_2 production are glassy carbon (GC), graphite and mercury electrodes. Among these working electrodes, mercury electrodes have a large overpotential for direct proton reduction at the electrode, which is an ideal electrode to avoid over-evaluating the efficiencies of catalysts. The reference electrodes frequently employed are Hg/Hg_2Cl_2 in a KCl saturated aqueous solution (a saturated calomel electrode, SCE), Ag/AgCl in a KCl saturated aqueous solution and $Ag/AgNO_3$ at different concentrations in CH_3CN. The potentials recorded *versus* these reference electrodes are often converted either to the normal hydrogen electrode (NHE) or to the ferricinium/ferrocene (Fc^+/Fc) couple for the comparison of electrocatalytic results obtained in different laboratories. The conversion constants between different reference electrodes in CH_3CN have been given in the literature.[14,15] Most of the conversion constants given in different literature reports are similar, but a correction for the conversion of the potential *vs.* NHE to that *vs.* Fc^+/Fc are quite different (−630 mV compared to −400 mV). The potentials mentioned in this perspective are referred to Fc^+/Fc unless otherwise noted. Potentials *vs.* other reference electrodes in CH_3CN were converted to potentials *vs.* Fc^+/Fc using the correction data given in the literature and potentials *vs.* SCE or Ag/AgCl in a KCl saturated aqueous solution were converted to potentials *vs.* NHE using the corrections of −241 mV and −197 mV, respectively.[15]

Good H_2-evolving electrocatalysts should work with a high catalytic activity and low overpotential, as well as being cheap and robust. The catalytic activity and the overpotential are two inseparable criteria for evaluating catalyst systems used for electrochemical H_2 production. In general, for the earth-abundant metal molecular catalysts reported to date, highly active catalysts tend to work at large overpotentials and catalysts working with small overpotentials usually display low catalytic activities. There are only a few exceptions, which will be described in subsections 3.1 and 3.4.

It should be noted that the TOFs reported in the literature are obtained by different methods. When the reduced protons come from an acid, the catalytic activities of homogeneous electrocatalysts are sometimes expressed as i_c/i_p, where i_c is the peak current in the presence of an acid and i_p is the peak current in the absence of an acid. As the concentration of the acid and the scan rate apparently influence the i_c/i_p ratio, comparison of the catalytic activities of different electrocatalysts using i_c/i_p ratios should be made on the basis of the same working electrode and similar experimental conditions. Evans, Glass and Lichtenberger employed the following equation (eqn (1)) to evaluate the catalytic efficiencies (C.E.) of electrocatalysts measured under comparable conditions,[15] provided that the reduction of the catalysts occurs *via* a single-electron process. For a double-electron process, i_p should be divided by two.

$$\text{C.E.} = \frac{i_c/i_p}{C_{HA}/C_{cat}} \qquad \begin{array}{l} C_{HA} = [\text{acid}] \\ C_{cat} = [\text{catalyst}] \end{array} \qquad \text{(eq 1)}$$

In addition to the i_c/i_p ratios and the C.E. values, TOFs have frequently been used to evaluate the catalytic activity of molecular catalysts. The TOFs for H_2-evolving electrocatalysts reported in the literature are generally given in different ways. One way is to calculate TOFs from i_c/i_p ratios according to the following equation (eqn (2)) for first-order or pseudo-first-order catalytic systems in the acid concentration-independent region:[16]

$$\frac{i_c}{i_p} = \frac{n}{0.4463}\sqrt{\frac{RTk_{obs}}{Fv}} \qquad \text{(eq 2)}$$

Here n is the number of electrons involved in the catalytic production of one molecule of H_2, R is the gas constant, T is the temperature in K, F is Faraday's constant, v is the scan rate in V $s^{-1}$and k_{obs} is the observed rate constant. In the acid-independent region, if k_{obs} is a first-order rate constant against the catalyst, the k_{obs} value is equivalent to the TOF of the catalyst with a unit of s^{-1}. The other method is to determine TOFs from controlled potential electrolysis experiments. Bulk electrolysis experiments can provide useful and credible data including: 1) the Faradaic efficiency, which shows how many electrons are effectively used in the proton reduction to H_2; 2) the total turnover number (TON), which is often used to show the stability of molecular catalysts. When the reduced protons come from water (in the absence of an acid), the catalytic activities of homogeneous electrocatalysts are usually expressed by the TOFs obtained from controlled potential electrolysis experiments. It should be noted that the TOFs determined from bulk electrolysis experiments are limited by the constant of the electrolysis cell and not by the catalytic steps. The actual catalytic rate in the kinetic sense cannot be measured using this technique.

The overpotential is another most important criterion for assaying an electrocatalyst. It is defined as the difference between the potential at which the catalytic reduction occurs and the standard potential ($E^\circ(HA/H_2)$) for the reduction of the acid or water under the operating conditions.[17,18] Because the potentials of the catalytic peaks are given in three ways (at the onset, the half-wave or the pinnacle of the peaks; herein we express the potentials given in these three ways as E_{on}, $E_{p/2}$ and E_p in the following sections), overpotentials are also given in different ways in the literature and can be calculated from $|E_{on} - E^\circ_{HA/H2}|$, $|E_{p/2} - E^\circ_{HA/H2}|$ and $|E_p - E^\circ_{HA/H2}|$. The overpotential calculated by $|E_p - E^\circ_{HA/H2}|$ overestimates the true overpotential and the one calculated by $|E_{on} - E^\circ_{HA/H2}|$ underestimates the overpotential. The recommended method is to use the half-wave potential of the catalytic wave to calculate the overpotential using $|E_{p/2} - E^\circ_{HA/H2}|$ for the catalyst systems working in acidic media. But, for a catalyst working in a neutral aqueous solution, the overpotential has to be calculated using $|E_{on} - E^\circ_{HA/H2}|$ because the catalytic peak grows continuously and the $E_{p/2}$ value cannot be determined from the peak.

The $E^\circ(HA/H_2)$ values in CH_3CN and DMF for various acids have been given in the literature.[17] To attain exact values of $E^\circ(HA/H_2)$, the homoconjugation phenomenon of acids in organic solvents must be considered. The homoconjugation phenomenon means that the conjugate base could be stabilized by hydrogen bonds to the acid, leading to an increase of the acidity of this acid. As the homoconjugation effect of the acid and its conjugate base in organic solvents, especially CH_3CN, has not been taken into account in the determination of $E°(HA/H_2)$, an overestimation of the value of $E°(HA/H_2)$ or, in another words, the underestimation of the overpotentials for electrocatalysts, may happen. The homoconjugation phenomena of many acids in organic solvents have been well discussed by Artero and Fontecave.[18]

In addition to the catalytic activity, overpotential and durability, the mediums and proton sources used for the H_2-evolving catalyst systems are also important factors to evaluate the homogeneous electrocatalysts in terms of their practical applications. Most of the reported H_2-evolving molecular electrocatalysts work in organic solvents, such as CH_3CN, DMF, CH_2Cl_2 and THF, in the presence of various acids. Although more than a hundred earth-abundant metal complexes are capable of electrochemically catalyzing the reduction of protons from acids to H_2, the known catalysts that can work efficiently *in aqueous solutions* are very limited. The molecular catalysts so-far reported for the electrochemical production of H_2 in aqueous solutions generally work with large overpotentials or with low Faradaic yields (see Section 4). It is still a great challenge to develop electrocatalysts that comprise only earth-abundant elements, work in water without the requirement of any organic solvents and with water as the proton source, and produce H_2 with a high activity at a low overpotentials over a long period of time.

3 The electrocatalytic H_2 production with earth-abundant metal complexes *in organic solvents*

In the following subsections, we divide the electrocatalysts into three categories according to the metal centers of the catalysts and the acids employed in the electrochemical H_2 production. Herein, the denotations of strong acids, moderate acids and weak acids are, respectively, as follows: $pK_a < 10$, $10 \leq pK_a \geq 15$ and $pK_a > 15$ (all pK_a values given here are determined in CH_3CN).

3.1 Nickel-based catalysts *with strong acids as the proton source*

Nickel complexes with base-containing diphosphine ligands (Fig. 1) are the most effective and robust molecular catalysts with overpotentials in the range of 0.2 to 0.7 V for electrochemical H_2 production in organic solvents with strong acids (HOTf and [(DMF)H]OTf) and substituted anilinium derivatives, as proton sources. In contrast, the reported cobalt- and iron-based catalysts are prone to decompose in the presence of strong acids. The efficiencies for electrochemical H_2 production employing nickel complexes with base-containing diphosphine ligands in CH_3CN are summarized in Table 1. The values of k_{obs} were calculated based on the ratios of i_c/i_p according to eqn (2) and the overpotentials were determined with the half-wave potentials ($E_{p/2}$) using the method of Evans.[17]

In 2002, DuBois and co-workers found that nickel complex **1** with two chelating 1,3-diethylphosphapropane (depp) ligands could reversibly cleave H_2 in the presence of 2,3-dichloroaniline to form a nickel hydride and the protonated dichloroaniline, indicating heterolytic cleavage of the H–H bond.[19] Inspired by the N-centred three atom bridge of the [FeFe]-hydrogenase active site ([FeFe]–H_2ase), an amine base was incorporated in the backbone of the diphosphine ligand to facilitate the proton transfer rate.[20] Coordination of two $Et_2PCH_2N(Me)CH_2PEt_2$ (PNP) ligands to the nickel ion **2** (Fig. 1) causes a 0.65 V negative shift of the potential for H_2 oxidation, as compared to that of

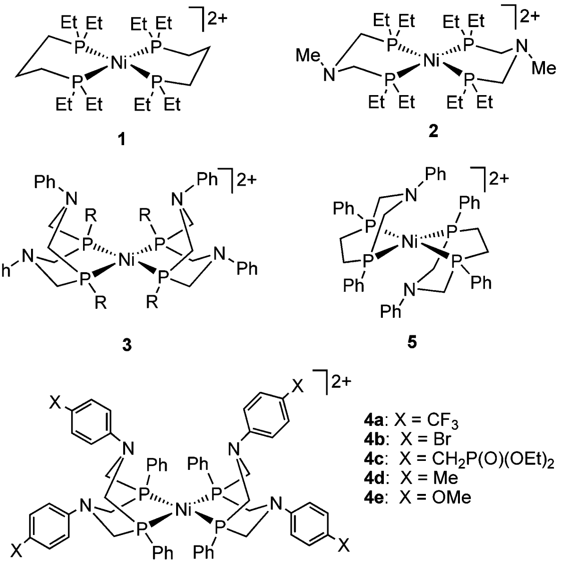

Fig. 1 DuBois' nickel(II) complexes with amine base-containing diphosphine ligands used as catalysts for electrochemical H_2 production.

Table 1 Electrocatalytic H_2 production by nickel complexes with base-containing diphosphine ligands in CH_3CN with different strong acids as proton sources

Catalyst	Acid concentration	OP[a]	k_{obs}[b]	Ref.
HOTf ($pK_a = 2.6$, $E°(HA/H_2) = -0.29$ V)				
3	0.10 M	0.57 V	130 s^{-1}	21
[2,6-$Cl_2C_6H_3NH_3$](OTf) ($pK_a = 5.0$, $E°(HA/H_2) = -0.44$ V)				
3	0.031 M (0.63 M H_2O)	0.37 V	160 s^{-1}	24
4b	0.044 M (0.14 M H_2O)	0.36 V	140 v	24
4c	0.051 M (0.30 M H_2O)	0.35 V	420 s^{-1}	24
$[(DMF)H]^+OTf$ ($pK_a = 6.1$, $E°(HA/H_2) = -0.50$ V)				
3	0.25 M	0.30 V	590 s^{-1}	24
3	0.28 M (0.03 M H_2O)	0.32 V	720 s^{-1}	24
4a	0.21 M (0.27 M H_2O)	0.30 V	120 s^{-1}	24
4b	0.43 M (0.27 M H_2O)	0.29 V	1040 s^{-1}	24
4c	0.35 M	0.20 V	500 s^{-1}	24
4c	0.35 M (0.55 M H_2O)	0.37 V	1850 s^{-1}	24
4d	0.30 M (0.05 M H_2O)	0.36 V	770 s^{-1}	24
4e	0.24 M (0.08 M H_2O)	0.33 V	480 s^{-1}	24
5	0.20 M	0.63 V	3.3×10^4 s^{-1}	16
5	0.43 M (1.2 M H_2O)	~0.63 V	1.06×10^5 s^{-1}	16
[4-$NCC_6H_4NH_3$](BF_4) ($pK_a = 7.5$, $E°(HA/H_2) = -0.58$ V)				
3	0.12 M (1.1 M H_2O)	0.33 V	72 s^{-1}	24
4c	0.20 M (2.4 M H_2O)	0.29 V	210 s^{-1}	24
4d	0.042 M (1.0 M H_2O)	0.35 V	94 s^{-1}	24
4e	0.05 M (2.0 M H_2O)	0.33 V	90 s^{-1}	24

[a] OP = overpotential = $|E_{p/2} - E°_{HA/H2}|$. [b] The values of k_{obs} were calculated by i_c/i_p in the acid-independent region according to eqn (2).

1 bearing depp ligands, but with a low reaction rate. In order to position the pendant amine base close to the nickel centre and slow the swing of the PCNCP bridge in the nickel complexes, the 1,5-diaza-3,7-diphosphacyclooctanes (P_2N_2) were designed as the ligands of nickel complexes **3** and **4a–4e** (Fig. 1).[21–24]

Among the tested acids, such as HOTf, anilinium derivatives, 1 : 1 DMF : [(DMF)H](OTf) and [(DMF)H](OTf), protonated dimethylformamide, [(DMF)H](OTf), proved to be the proper acid for electrochemical H_2 production considering the stability and activity of nickel complexes. Complex **3** is a highly efficient electrocatalyst for H_2 production, with a TOF of up to 590 s^{-1} and an overpotential of ~0.3 V using protonated dimethylformamide, [(DMF)H](OTf), as the proton source in CH_3CN. The high catalytic rates observed with these complexes are attributed to the well positioned amine base in the second coordination sphere of the catalyst to serve as a proton relay in the cleavage and formation of the H–H bond.

Furthermore, studies on a series of nickel complexes **4a–e** reveal that the substituent X in the *para* position of the *N*-aryl substituent has a considerable influence on the catalytic activity.[24] The catalytic activities of H_2 production increase from 310 to 740 s^{-1} as the electron-withdrawing ability of the X substituent increased from OMe to Br, with overpotentials in the range of 0.28 to 0.34 V using [(DMF)H](OTf) as the acid in CH_3CN, while with strong electron-withdrawing group CF_3 at the *para* position of the *N*-aryl substituent, the TOF reduced to 95 s^{-1} with an overpotential of 0.30 V. An unusual phenomenon that the catalytic activities increase as the potentials of the catalysts become more positive was found for the series of nickel complexes **4a–d**. Addition of a small amount of water greatly enhances the catalytic activity. The phosphonate functionalized complex **4c** ($X = CH_2P(O)(OEt)_2$) gave the highest TOF (1850 s^{-1}) with an overpotential of 0.37 V using [(DMF)H](OTf) as the acid (350 mM) with the addition of water (550 mM). Under similar conditions, the complex **4b** (X = Br) displayed TOFs of up to 1040 with an overpotential of 0.29 V and the TOF of **3** (X = H) is up to 720 s^{-1} with an overpotential of 0.32 V.

The mechanism of electrocatalytic H_2 generation by these nickel complexes has been well studied by DuBois and co-workers, which revealed that three isomers, **A**, **B** and **C**, of the intermediates are formed by a two electron reduction and double protonation of **3a** (Fig. 2).[25] Among them, only isomer **A** is active in the catalytic cycle. To avoid formation of isomers **B** and **C**, one of the pendant N atoms is removed from the cyclic diphosphine ligand to forge the seven-membered cyclic ligand, 1-aza-3,6-diphosphacycloheptane (P_2N). This small but significant modification of the structure of the diphosphine ligand greatly improved the catalytic activity of the nickel complex **5** for electrocatalytic H_2 production.[16] The TOF for **5** is enhanced to 33,000 s^{-1} with an overpotential of 0.63 V using [(DMF)H](OTf) as an acid (0.43 M) in CH_3CN as compared to 590 s^{-1} with an overpotential of 0.30 V for **3**. The TOF jumps from 720 s^{-1} for **3** to 106,000 s^{-1} for **5** with the addition of an optimal amount of water under similar conditions, accompanied by an increase of the overpotential from 0.32 to 0.63 V. After the maximum current enhancement was reached, the further addition of water resulted in a decrease of the catalytic activity. The advantages of the nickel catalyst **5** are its extremely high activity and good stability for electrocatalytic H_2 production, while the disadvantages are that the H_2-evolving reaction occurs with a large overpotential (>600 mV) and has to be carried out in non-aqueous solution using strong acids as a proton source.

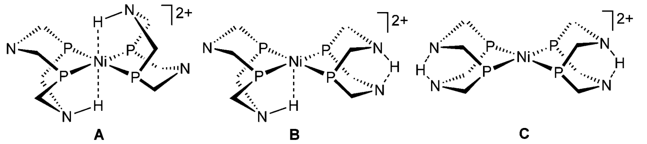

Fig. 2 Double protonated nickel(0) intermediates (**A**, **B** and **C**) involved in the production of H_2 catalyzed by **3** and **4**. Groups on the N and P atoms of the ligands are omitted for clarity.

In general, DuBois' nickel complexes effectively mimic the structural characters of [FeFe]- and [NiFe]-hydrogenases by introducing and fixing an internal base close to the metal centre. Studies on the catalytic properties of these amine base-containing nickel complexes reveal the important role of pendant amines as proton relays in the aspect of accelerating the electrocatalytic proton reduction. A deep insight into the mechanism of the catalytic H_2-generation reaction helps chemists to understand the correlation between the structure and activity of catalysts and guides researchers in the design of more efficient catalysts. It is expected that the performance of nickel-based electrocatalysts in aqueous media could be improved and the overpotentials could be reduced by modification of the amine base-containing cyclic diphosphine ligands in further studies.

3.2 Cobalt-based catalysts *with strong and moderate acids as the proton source*

Cobalt complexes as catalysts for electro- and photochemical H_2 generation have drawn great attention in recent years due to their rich redox chemistry and catalytic power. According to the ligands, the cobalt complexes used as H_2-evolving electrocatalysts are divided into eight classes: N_4-macrocyclic complexes,[26,27] hexaamino complexes,[28] porphyrin complexes,[29,30] phthalocyanine complexes,[31] cyclopentadienyl complexes,[32,33] cobalt glyoxime complexes,[9,10] polypyridine complexes[34] and cobalt complexes with one or two base-containing diphosphines.[35] Here, we will focus on the electrocatalytic production of H_2 from strong and moderate acids by cobalt glyoxime complexes (**6–10**, Fig. 3), as well as polypyridine complex (**11**) and cobalt complex (**12**) with a base-containing diphosphine reported in recent years. The related electrocatalytic results are listed in Table 2.

The application of cobaloximes as catalysts for electro- and photochemical proton reduction has been widely investigated in recent years, not only due to their convenient preparation but also their good catalytic activities and modest to small overpotentials. All studies on the homogeneous electrochemical proton reduction with cobaloximes as catalysts were carried out in organic solvents, such as CH_3CN, DMF and 1,2-$C_2H_4Cl_2$. Cobaloxime complexes (**6–9**) either with $O–BF_2\cdots O$ or $O–H\cdots O$ bridges display relatively small overpotentials (<0.3 V) for proton reduction in the presence of strong and moderate acids.[36–40] These cobaloxime complexes are among the most efficient catalysts reported to date for the reduction of protons from acids in non-aqueous solvents in terms of overpotential and catalytic frequency.

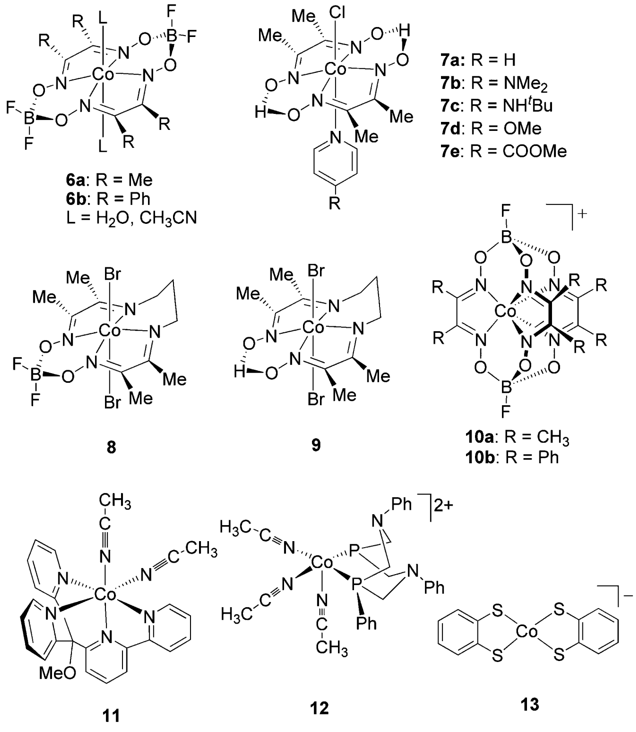

Fig. 3 Structures of cobalt-based catalysts **6–13**.

The O–$BF_2\cdots$O bridged complex **6a** catalyzes proton reduction at a potential of −0.94 V in the presence of CF_3COOH, corresponding to a relatively small overpotential (~50 mV) with a low efficiency.[36,37] This overpotential is probably underestimated because, when CF_3COOH is used as the acid, there is a large homoconjugation constant that is not taken into account when the overpotential is calculated.[18] Using *p*-cyanoanilinium as the proton source under identical conditions, the overpotential of electrocatalysis for **6a** is 0.2 V with a i_c/i_p ratio *ca.* 3.7 times as high as that observed in the presence of CF_3COOH. A nearly quantitative Faradaic yield and 20 TON h^{-1} were obtained by bulk electrolysis in CH_3CN at −1.11 V with **6a** as the catalyst and CF_3COOH as the proton source, and 46 TON was obtained at −0.94 V in 30 min with *p*-cyanoanilinium as the acid. Complex **6b** with phenyl groups in the glyoxime displays a very small overpotential with low activity for H_2 production with $HCl\cdot Et_2O$ as the proton source.

Cobalt(III) cobaloximes **7a–d** exhibit catalytic peaks at almost identical potentials (−1.40 to −1.45 V) for proton reduction in DMF in the presence of Et_3NHCl, indicating that changing the substituent in the axial pyridine of the cobaloxime complexes does not significantly influence the catalytic potential of cobaloxime complexes. Bulk electrolysis on a graphite electrode at −1.34 V in 1,2-$C_2H_4Cl_2$ with **7a** as the catalyst and $Et_3NH(BF_4)$ as the proton source gives 85–100% Faradaic yield with ~100 TON in 2.5 h.[38]

The stability of a catalyst is one of the crucial issues for the application of the catalyst. Complex **6a** is stable in the presence of weak acids, such as $Et_3NH(BF_4)$ and Et_3NHCl in CH_3CN, but it gradually decomposes in the presence of moderate and strong acids, such as CF_3COOH and *p*-cyanoanilinium tetrafluoroborate, and strong acids, such as $HCl\cdot Et_2O$ and $HBF_4\cdot Et_2O$, hydrolyze **6a** within a few minutes in CH_3CN. Therefore, it is imperative to improve the stability of cobaloxime catalysts. The structurally modified cobaloxime complexes **8** and **9** were prepared, in which one of the O–$BF_2\cdots$O or O–$H\cdots$O bridges was replaced by a $CH_2CH_2CH_2$ chain to increase the stability of the cobaloxime complexes. These complexes are also electrocatalytically active for H_2 evolution, with similar overpotentials (0.24 V for **8** and 0.2 V for **9**) as have been reported for **6a** in the presence of *p*-cyanoanilinium.[39] Complexes **8** and **9** show high Faradaic efficiencies (92–100%) with 20 and 40 TONs of H_2-evolution, respectively, in 3 h electrolysis at a graphite electrode with an applied potential of −0.82 V for **8** and −0.78 V for **9** using *p*-cyanoanilinium as an acid in CH_3CN. It is noted that the electrocatalytic potential of **9** apparently changes in the presence of different acids (Table 2). Although the efficiencies of electrocatalytic H_2 evolution are slightly lower than that (50 TON) obtained for their analogue, **6a**, by electrolysis at −0.80 V, complexes **8** and **9**, with one side bridged by a propylene group, display apparently better stability during electrolysis under acidic conditions as compared to conventional cobaloxime complex **6**. For example, no evidence for the decomposed species of **8** was spectroscopically detected from a millimolar solution of **8** in the presence of 30 equiv. of *p*-cyanoanilinium tetrafluoroborate in CH_3CN over two weeks, while **6a** was decomposed under identical conditions with a half-life of 15 h. When cobalt clathrochelate complexes **10a** and **10b** were used as electrocatalysts in the presence of a strong acid ($HClO_4$) relatively low efficiencies of H_2 production with large overpotentials (0.53–0.83 V) and poor Faradaic yields (10–35%) were observed, possibly due to the lack of a labile ligand at the metal centre.[41]

In addition to the cobalt complexes of glyoximes, cobalt complexes with polypyridine and base-containing diphosphine ligands (Fig. 3) were used as catalysts for the electrochemical production of H_2 from moderate acids.[34] Complex **11** displays a catalytic peak at *ca.* −1.3 V in CH_3CN with CF_3COOH as the proton source, corresponding to a overpotential of 0.41 V. The controlled potential experiment carried out at −1.40 V with 60 mM CF_3COOH confirmed the production of H_2 with a ~99% Faradaic yield and *ca.* 40 mol H_2 per mole of **11** per h. The cobalt complex **12** with only one positioned pendant amine base in a single cyclic diphosphine ligand is also an efficient catalyst for electrochemical H_2 production.[35] It displays catalytic activity up to 90 s^{-1} with an overpotential of 0.29 V using 4-bromoanilinium tetrafluoroborate as a proton source in CH_3CN. The efficiency of the cobalt complex **12** for proton reduction is lower than those of the above-mentioned nickel complexes. Very recently, Eisenberg and co-workers reported a cobalt dithiolene complex **13** for the electrocatalytic reduction of protons.[42] The controlled potential electrolysis experiment at −1.0 V *vs.* SCE in 1 : 1 CH_3CN/H_2O gave a Faradaic yield of >99%.

The mechanisms of the H_2-evolving reaction catalyzed by cobalt-based complexes have been studied theoretically by several groups. Mechanisms with $Co^{III}H$ and $Co^{II}H$ as key intermediates were proposed.[43–46] Scheme 1 shows the catalysis of proton reduction to H_2 by cobalt complexes associated with the formation of the $Co^{III}H$ species *via* protonation of the reduced cobalt(I) species. The $Co^{III}H$ intermediate yields H_2 by protonolysis or bimolecular pathways. The other plausible mechanisms, EECC and ECEC (C = chemical, E = electrochemical,

Table 2 Electrocatalytic H_2 production by cobalt-based catalysts with strong and moderate acids as proton sources[a]

			Bulk electrolysis		
Catalyst	Catalytic potential (E_p)	OP[b]	Applied potential	efficiency	Ref.
$HClO_4$ ($pK_a = 2.1$, $E°(HA/H_2) = -0.26$ V)					
10a	−1.09 V	0.83 V	−1.24 V[c]	FY 35%[d] ~1.5 TON (0.5 h)	41
10b	−0.79 V	0.53 V	−0.94 V[c]	FY 10% <0.5 TON (0.5 h)	41
[4-$NCC_6H_4NH_3$](BF_4) ($pK_a = 7.5$, $E°(HA/H_2) = -0.58$ V)					
6a	−0.78 V	0.20 V	−0.94 V[c]	45 TON (0.5 h)	37
8	−0.82 V	0.24 V	−0.82 V[e]	FY ~ 100% 20 TON (3 h)	39
9	−0.78 V	0.20 V	−0.78 V[e]	FY 92% 40 TON (3 h)	39
HOTs ($pK_a = 8.7$, $E°(HA/H_2) = -0.65$ V)					
8	−0.85 V	0.20 V	−0.85 V[e]	FY ~ 100% 15 TON (3 h)	39
9	−0.83 V	0.18 V	−0.83 V[e]	FY 50% 4 TON (3 h)	39
$HCl\cdot Et_2O$ ($pK_a = 8.9$, $E°(HA/H_2) = -0.67$ V)					
6b	−0.67 V	0 V	−0.76 V[f]	FY 90% 11 TON (1 h)	36
[4-$BrC_6H_4NH_3$](BF_4) ($pK_a = 9.4$, $E°(HA/H_2) = -0.69$ V)					
12	−0.99 V[g]	0.30 V[h]	−1.1 V[f]	FY ~ 100% k_{obs} 90 s^{-1}	35
CF_3COOH ($pK_a = 12.7$, $E°(HA/H_2) = -0.89$ V)					
6a	−0.94 V	0.05 V	−1.11 V[f]	FY ~ 100% 20 TON (1 h)	36
8	−0.89 V	~0 V	−0.89 V[e]	FY 90% 7 TON (3 h)	39
9	−1.10 V	0.21 V	−1.0 V[e]	FY 91% 20 TON (3 h)	39
11	~−1.3 V	0.41 V	−1.4 V[f]	FY ~ 99% 40 h^{-1}	34
13	−1.01 V	~0.12 V	−1.39 V[f]	FY > 99%	42
Et_3NHCl ($pK_a = 18.7$, $E°(HA/H_2) = -1.25$ V)					
6a	−1.87 V	0.62 V	−1.39 V[c]	~4 TON (1 h)	37
7a–d	−1.40 to −1.45 V (DMF)	0.15–0.20 V			38

[a] Electrocatalytic reactions were carried out in CH_3CN unless otherwise noted with a GC working electrode. [b] OP = overpotential = $|E_p - E°_{HA}|$ except for **12**. [c] Hg pool. [d] FY = Faradaic yield. [e] Graphite electrode. [f] GC electrode. [g] $E_{p/2}$. [h] OP = $|E_{p/2} - E°_{HA}|$.

Scheme 2) mechanisms, proceed *via* a $Co^{II}H$ intermediate formed either by reduction of the $Co^{III}H$ or protonation of the Co^0 species.

Although the functions of the internal bases in iron- and nickel-based molecular catalysts have been extensively studied, the base-containing cobalt catalysts have not been found in the literature. It would be interesting to study this further to design novel cobalt-based catalysts bearing an internal base close to the cobalt centre and to explore the function of the pendant base of a cobalt catalyst in electrochemical H_2 production. The catalytic activities of H_2 production by cobalt complexes might be improved by introduction of an internal base.

3.3 [NiFe]–H_2ase mimics *with moderate acids as the proton source*

The unveiling of the structures of [NiFe]- and [FeFe]-hydrogenase ([FeFe]–H_2ase) active sites inspired an extensive interest in the chemistry of NiFe and FeFe dithiolate complexes. The [NiFe]- and [FeFe]-hydrogenases can catalyze both H_2 activation and formation. The catalytic activity of the [FeFe]–H_2ase for H_2 generation is up to 9000 molecules of H_2 s^{-1} per site with an overpotential less than 100 mV in aqueous solution at pH 7 and the activity of [NiFe]–H_2ase is *ca.* 500 molecules of H_2 s^{-1} per site with an onset potential of −0.35 V *vs.* NHE at pH 6.[16,47] Although hydrogenases are much more efficient for H_2

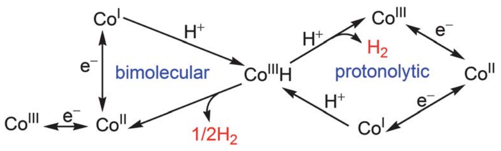

Scheme 1 Proposed mechanisms for proton reduction catalyzed by cobalt complexes with $Co^{III}H$ as a key intermediate.

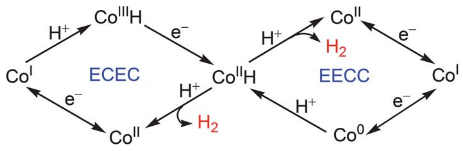

Scheme 2 Proposed mechanisms for proton reduction catalyzed by cobalt complexes with $Co^{II}H$ as a key intermediate.

production as compared to reported hetero- and homogeneous catalysts, they are not ideally suited for large-scale and long-term use because of the strictly limited reaction conditions due to the instability of the enzymes in aerobic environments. In the past decade, many chemists have been engaging in the study of structural and functional biomimics of [FeFe]- and [NiFe]–H_2ases, aiming at the development of bioinspired electro- and photocatalysts for H_2 production,[48,49] even though at present it seems too difficult to attain biomimic H_2-evolving catalysts with efficiencies and overpotentials satisfying the requirements for applicable devices. It is expected that, with a better understanding of the mechanisms of H_2 formation and uptake at the active sites of hydrogenases and with an insight into the basic structure–microenvironment–function relationship of the enzyme centre, well-designed FeFe and NiFe mimics could function as highly efficient catalysts with small overpotentials for H_2 generation under mild conditions.

Rauchfuss and co-workers reported the first examples of NiFe thiolato hydrides (**14a–d**, Fig. 4),[50,51] which mimic the $NiFeS_2(\mu\text{-}H)$ core in the active site of [NiFe]–H_2ases. Complexes **14a–d** are catalytically active for electrochemical H_2 production in CH_2Cl_2 with CF_3COOH as a proton source. The electrocatalytic results are given in Table 3.

It should be mentioned that the overpotentials listed in Table 3 are probably significantly underestimated because the homoconjugation of CF_3COOH could be orders of magnitude larger in CH_2Cl_2 compared to CH_3CN. Complexes **14b–d**, with a phosphine coordinating to the Fe centre, display similar efficiencies under identical conditions. The acid-independent rate constant for **14b–d** is 50 s^{-1} for H_2 generation from CF_3COOH. The catalytic potential of **14a** containing an $Fe(CO)_3$ unit is about 100 mV less negative than those of **14b–d** and, accordingly, with a lower acid-dependent rate constant (20 s^{-1}). A new catalytic peak at $E_{p/2} = -1.15$ V, 200 mV less negative than the reduction potential of **14d**, was observed upon addition of CF_3COOH to the solution of **14d**. The new catalytic peak is attributed to the pyridine N-protonated complex [**14d**H]$^+$, which affords a k_{obs} of 50 s^{-1} in the acid-independent region. In general, NiFe complexes **14a–d** exhibit milder catalytic potentials and similar catalytic activities as compared to FeFe mimics for electrochemical reduction of protons from CF_3COOH in organic solvents.

The other two [NiFe]–H_2ase mimics (**15** and **16**, shown in Fig. 5) were reported by Artero and co-workers.[52,53] Complex **15**, with a S_4 set of ligands around nickel and a cyclopentadienyl ligand on the iron center, catalyzes the hydrogen evolution in DMF in the presence of CF_3COOH at *ca.* −1.73 V, corresponding to an overpotential of 730 mV. The bulk electrolysis experiment showed 20 TON of H_2 evolution in a 4 h experiment with a Faradaic yield of 72% at a controlled potential of −1.83 V in a DMF solution of **15** (7 μmol) and CF_3COOH (0.7 mmol) on a Hg-pool cathode. The rate of catalysis (5 TON h^{-1}) is sustained over the 4 h electrolysis experiment, indicating that the catalyst has good stability in the catalytic cycle. The NiMn complex **16**, having the same nickel moiety as **15**, displays a similar catalytic activity to that of **15** for the electrochemical reduction of protons from CF_3COOH to H_2 in DMF at −1.81 V ($E_{p/2}$), corresponding to an overpotential of 860 mV. A bulk electrolysis experiment of the CF_3COOH (0.1 M) solution in DMF at a controlled potential of −1.82 V in the presence of **16** (1 mmol) afforded 15.8 TON of H_2 evolution in a 4 h experiment with a Faradaic yield of 94%. DFT studies suggest that **15** and **16** mediate H_2 evolution in a heterolytic fashion from bridging hydride intermediates with a structure similar to that of the Ni–C active site of [NiFe]–H_2ases.

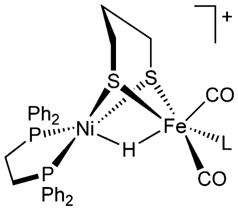

14a: L = CO
14b: L = $P(OPh)_3$
14c: L = PPh_3
14d: L = PPh_2Py

Fig. 4 The structures of NiFe thiolato hydrides **14a–d**.

Table 3 Electrocatalytic H_2 production by [NiFe]–H_2ase mimics with CF_3COOH as a proton source[a]

Catalyst	Catalytic potential ($E_{p/2}$)[b]	OP[c]	k_{obs}[d]	Ref.
CF_3COOH (pK_a = 12.7, $E°(HA/H_2) = -0.89$ V)				
14a	−1.20 V	0.31 V	20 s^{-1}	51
14b	−1.32 V	0.43 V	50 s^{-1}	51
14c	−1.30 V	0.41 V	50 s^{-1}	51
14d	∼−1.3 V	∼0.4 V	50 s^{-1}	51
[**14d**H]$^+$	−1.15 V	0.26 V	50 s^{-1}	51

[a] Electrocatalytic reactions were carried out in CH_2Cl_2. [b] GC electrode. [c] OPs were estimated by $E°(HA/H_2)$ for CF_3COOH in CH_3CN. [d] The values of k_{obs} were calculated by i_c/i_p in the acid-independent region according to eqn (2).

3.4 [FeFe]–H_2ase mimics *with moderate and weak acids as the proton sources*

Although a strong acid (H_2SO_4) was employed in the first example of electrochemical H_2 evolution catalyzed by a biomimetic diiron dithiolate complex,[54] which gave 6 turnovers of H_2 production with an overpotential of −0.82 V in the bulk electrolysis experiment at −1.4 V in CH_3CN, strong acids such as H_2SO_4, HBF_4, $HClO_4$, HCl and HOTf are not generally suitable for [FeFe]–H_2ase mimics because of their large overpotentials (0.7–2.0 V) and their instability in the presence of strong acids.[15]

There are only a few examples for H_2 production employing moderate acids (pK_a = 10–15), giving medium efficiencies with

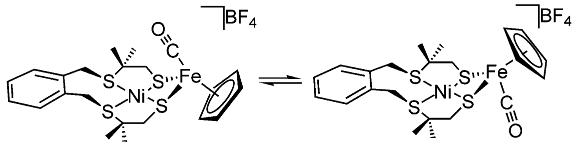

15

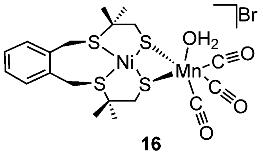

16

Fig. 5 The structures of the NiFe (**15**) and NiMn (**16**) complexes.

overpotentials in the range of −0.4 to −1.2 V in CH_3CN.[55–57] The electrocatalytic results of diiron complexes **17–20** (Fig. 6) for the reduction of protons from CF_3COOH are given in Table 4.

In most cases, weak acids (pK_a > 15, $ClCH_2COOH$, $NCCH_2COOH$, Et_3NH^+, HOAc and C_6H_5COOH) have been used as proton sources for the electrocatalyst systems of diiron complexes. The overpotentials vary in the range of −0.2 to −1.0 V in the presence of these weak acids in CH_3CN.[15] Although more than seventy examples were reported for electrocatalytic H_2 production by diiron complexes in the presence of weak acids, there are limited data to draw an intrinsic relationship between the structures and the electrocatalytic efficiencies of the [FeFe]–H_2ase mimics as the results were obtained using different electrodes and acids with various concentrations of catalysts and acids in different solvents. To gain insight into the influence of ligands on the electrocatalytic properties of diiron complexes in proton reductions, we only compare the electrocatalytic results using HOAc in CH_3CN (Tables 5 and 6). The data in each table are divided into several sets. The compared data of each set come from the experiments performed by the same group with a weak acid (HOAc) using the same concentrations of acid and catalyst in CH_3CN. The structures of the diiron complexes reported in Tables 5 and 6 are shown in Fig. 7.

Except **34**, the listed [FeFe]–H_2ase mimics in Fig. 7 each display two one-electron reduction events, ascribed to Fe^IFe^I/Fe^IFe^0 and Fe^IFe^0/Fe^0Fe^0 couples. Generally, the first reduction event of the all-CO [FeFe]–H_2ase mimics is inactive for electrocatalytic proton reductions in the presence of HOAc and the second reduction event is the catalytic peak with large overpotentials. The first reduction event becomes electrocatalytically active for H_2 generation with replacement of one or two COs by PR_3, *N*-heterocyclic carbene or another non-CO ligand. Therefore, compared to the corresponding all-CO diiron complex, introduction of a strong electron donating non-CO ligand to a [FeFe]–H_2ase mimic leads to an apparent decrease in both the overpotential and the efficiency (**22** *vs.* **21** in Table 5).[58,59] Comparison of the data, with **23** *vs.* **22**, **26** *vs.* **25**[60] and **28** *vs.* **27**,[61] indicates that further introduction of a second non-CO ligand results in a considerable increase in the overpotential and efficiency. Diiron complexes containing strong electron donating ligands display larger overpotentials and higher efficiencies than those bearing weaker electron donating ligands (**24** *vs.* **23** and **28** *vs.* **26**). The data of **29** and **30** show that the introduction of a chelating ligand, leading to the formation of an asymmetric disubstituted diiron complex, significantly enhances the efficiency with an increase of the overpotential to 0.8 V.[62]

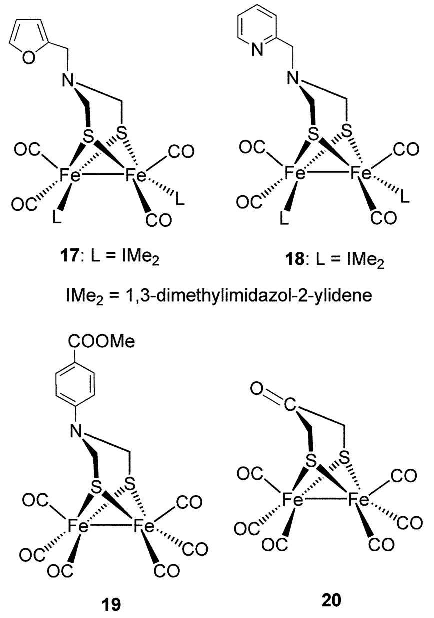

17: L = IMe$_2$

18: L = IMe$_2$

IMe$_2$ = 1,3-dimethylimidazol-2-ylidene

19

20

Fig. 6 The structures of diiron complexes **17–20**.

Table 4 Electrocatalytic H_2 production by [FeFe]–H_2ase mimics with F_3CCOOH as the proton source[a]

Catalyst	Catalytic potential (E_p)[b]	OP[c]	C.E.[d]	Ref.
F_3CCOOH (pK_a = 12.7, $E°$(HA/H_2) = −0.89 V)				
17	−1.51 V	0.62 V	0.29	55
18	−1.72 V	0.83 V	0.60	55
19	−1.60 V	0.71 V	0.34	56
20	−1.48 V	0.59 V	0.33	57

[a] Electrocatalytic reactions were carried out in CH_3CN. [b] GC electrode. [c] OP = overpotential = $|E_p - E°_{HA}|$. [d] The C.E. values are either cited from ref. 15 or calculated according to eqn (1).

Changing the dithiolato groups is another method to adjust the electronic properties of [FeFe]–H_2ase models. The first reduction potentials of Fe_2S_2 complexes are tuned in the range of −1.18 to −1.67 V for the all-CO complexes with different dithiolate bridges in CH_3CN.[15] Table 6 gives the electrocatalytic data for five all-CO [FeFe]–H_2ase mimics measured under similar conditions. It is noteworthy that compared to the efficiency of **31**, containing a SCH_2OCH_2S bridge, the C.E. of **32**, which features a more flexible bridge ($SCH_2CH_2OCH_2CH_2S$) is apparently increased, while the overpotential is only slightly increased from 0.74 to 0.82 V.[63,64] The set of **21** *vs.* **31** and **33**, which contain $CH_2CH_2CH_2$,[58] CH_2OCH_2,[63] and CH_2NRCH_2 bridges,[65] respectively, is another example of an increase in the efficiency accompanied by a decrease of the overpotential for proton reduction. Complexes **31** and **33**, with an O or N atom in the center of the bridge, display a higher efficiency with smaller overpotentials than complex **21**, which may possibly be caused by the internal base.

Complex **34** with a rigid and conjugate bridge exhibits quite different electrochemical properties to most [FeFe]–H_2ase mimics with flexible bridges. For example, while complex **34** is reduced to its dianion at −1.27 V ($E_{1/2}$) in a electrochemically reversible two-electron process in CH_3CN,[66,67] complex **21** displays the first one-electron reduction event at −1.65 V and the second irreversible reduction event at a potential that is 0.6 V more negative than the first reduction event.[58] The reduced species of such aromatic ring-bridged diiron complexes are strongly stabilized by the benzene bridge. Therefore, complex **34** is a more efficient and robust catalyst for electrochemical proton reductions as compared to the other diiron mimics.[68,69] The catalysis occurs at a potential where **34** itself shows no electroreduction event. In the presence of weak acids, the overpotentials are in the range of 0.44 to 0.77 V with moderate to high efficiencies for proton reduction catalyzed by **34**. For example, the C.E. of **34** is as high as 0.96 with an overpotential of 0.77 V in the presence of chloroacetic acid, which corresponds to efficient

Table 5 The influence of CO-displacement on the electrocatalytic properties of [FeFe]–H_2ase mimics[a]

Set	Complex	Non-CO ligand	E_p (V)	OP[b] (V)	C.E.[c]	[HOAc] (mM)	[Catalyst] (mM)	Ref.
I	**21**	—	−2.35	0.89	0.06	100	2.0	58
	22	PTA	−1.94	0.48	0.03	100	2.0	59
	23	2 PTA	−2.18	0.72	0.08	100	2.0	59
	24	2 PMe_3	−2.25	0.79	0.11	100	2.0	59
II	**25**	DAPTA	−1.83	0.37	0.43	4	1.0	60
	26	2 DAPTA	−2.0	0.54	0.65	4	1.0	60
III	**27**	PPh_2(2-Py)	−1.86	0.40	0.43	5	1.0	61
	28	PPh_2(2-Py) PMe_3	−2.20	0.74	0.70	5	1.0	61
IV	**29**	IMe_2[d]	−2.08	0.62	0.19	10	1.0	62
	30	IPyMe[e]	−2.30	0.80	1.10	10	1.0	62

[a] Conditions: a GC working electrode, a platinum wire counter electrode and a Ag/$AgNO_3$ (0.01 M in acetonitrile) reference electrode, in acetonitrile. [b] OP = overpotential = $|E_p - E^\circ_{HA}|$. [c] The C.E. values are either cited from ref. 15 or calculated according to eqn (1). [d] IMe_2 = 1,3-dimethylimidazol-2-ylidene. [e] IPyMe = 1-methyl-3-(2-pyridyl)imidazol-2-ylidene.

catalysis where the current is limited by the rate of diffusion of the acid to the electrode. In view of the merits of the mild reduction potential of **34** as compared to other [FeFe]–H_2ase mimics, the two-electron transfer process and the good stability of the reduced species, this family of [FeFe]–H_2ase mimics deserve further deep study of the electro- and photocatalytic H_2 production.

The mechanisms for electrochemical H_2 production catalyzed by diiron complexes depend on the basicity of diiron centers, the internal bases and the ligands in the catalysts, as well as the reaction conditions, such as the acids and media employed. Four possible pathways have been reported for electrocatalytic H_2 generation by diiron complexes, namely EECC, ECCE, CECE and CCEE (Scheme 3). The EECC mechanism has been proposed for electrochemical H_2 production with a weak acid (HOAc) in CH_3CN catalyzed by all-CO diiron complexes, while the ECCE mechanism has been proposed for the PR_3-substituted diiron complexes.[58] The CECE pathway is a plausible mechanism for the PR_3-substituted diiron complexes without an internal base when a stronger acid (HOTs) is employed as the proton source and the protonation occurs at the diiron center.[70] For catalysts containing an internal base, the CECE mechanism is also possible with an internal base as the proton relay, which is normally an amine base, if the pK_a of the acid used matches the basicity of the internal base.[71] In the presence of a strong acid (H_2SO_4) in CH_3CN, the H_2-evolving reaction catalyzed by (μ-pdt)[$Fe(CO)_2(PMe_3)$][$Fe(CO)_2(CN)$]$^-$ possibly proceeds by a CCEE mechanism.[54] In addition, the ECEC mechanism has been proposed for photochemical H_2 production catalyzed by diiron complexes,[72] but has not been assumed for the diiron-based electrochemical H_2-evolving catalyst systems.

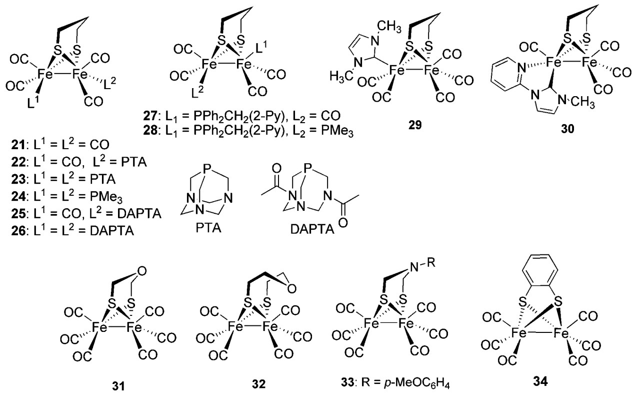

Fig. 7 The structures of [FeFe]–H_2ase mimics **21–34**.

4 Electrocatalytic H_2 production with earth-abundant metal complexes *in aqueous solutions*

4.1 Electrocatalytic production of H_2 *in acidic aqueous solutions*

4.1.1 With [FeFe]–H_2ase mimics as the catalysts. Water solubility, at least to a certain extent, is one of the desired properties for H_2-evolving catalysts, considering that the ultimate goal is to build H_2 production systems combining the proton reduction catalysts with a water oxidation system. Most iron-based molecular catalysts are only soluble in organic solvents. Therefore, studies on their electrocatalytic H_2 production are usually made in organic solvents, such as CH_3CN, DMF and THF, in the presence of various acids. Some efforts have been made to enhance the water solubility of diiron dithiolate

Table 6 The influence of changing the dithiolato group on the electrocatalytic properties of [FeFe]–H_2ase mimics[a]

Complex	E_p (V)	OP[b] (V)	C.E.[c]	[HOAc] (mM)	[Catalyst] (mM)	Ref.
31	−2.20	0.74	0.40	10	1.0	63
32	−2.28	0.82	0.91	10	1.0	64
33	−2.10	0.74	0.19	10	1.0	65
34[d]	−2.11	0.65	0.64	5	1.0	68,69

[a] Conditions: a GC working electrode (except **34**) in acetonitrile. [b] The same as those in Table 5. [c] The same as those in Table 5. [d] With a mercury film on a gold disk working electrode.

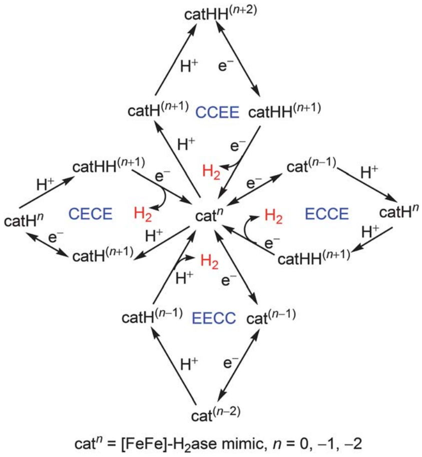

Scheme 3 Possible pathways for H_2 production catalyzed by [FeFe]–H_2ase mimics.

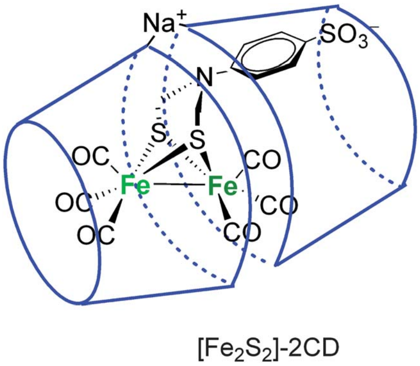

Fig. 8 The structure of a host–guest supramolecule with inclusion of an [FeFe]–H_2ase mimic into the cavity of β-cyclodextrin.

complexes by introducing hydrophilic phosphine ligands, such as PTA (1,3,5-triaza-7-phosphaadamantane),[59] DAPTA (3,7-diacetyl-1,3,7-triaza-5-phosphabicyclo[3.3.1]nonane),[60,73] $P(CH_2OH)_3$,[74] and $P(CH_2CH_2COOH)_3$.[75] Complexes [(μ-pdt){Fe(CO)$_3$}{Fe(CO)$_2$PTA}] (**22**) and [(μ-pdt){Fe(CO)$_2$PTA}$_2$] (**23**) show good solubility in CH_3CN/H_2O mixtures. They can catalyze the reduction of protons from HOAc in CH_3CN/H_2O (1 : 1) with overpotentials of 0.48 and 0.72 V, respectively. Diiron complexes containing the DAPTA ligand, an acetylated derivative of PTA, have much better water solubility than their PMe_3- and PTA-containing analogues. Accordingly, [(μ-pdt){Fe(CO)$_2$PTA}{Fe(CO)$_2$DAPTA}] and [(μ-pdt){Fe(CO)$_2$DAPTA}$_2$] (**26**) are capable of electrochemically reducing protons from HOAc in water at −1.3 *vs.* NHE.

Very recently, Darensbourg and co-workers reported a host–guest supramolecule (Fig. 8) with inclusion of an [FeFe]–H_2ase active site model into the cavity of β-cyclodextrin (β-CD) to mimic the protein environment of the [FeFe]–H_2ase enzymes.[76] The inclusion diiron complex has good solubility in water and displays a weak catalytic peak at −1.4 V *vs.* Ag/AgCl in the presence of HOAc in an aqueous NaCl solution. Despite the rapid exchange of the diiron complex in and out of the cyclodextrin in an aqueous solution, such a host–guest system is the first example mimicking the protein environment for a small molecule model of the [FeFe]–H_2ase active site.

Although near one hundred [FeFe]–H_2ase mimics have been reported for electrochemical H_2 generation, large overpotentials, low efficiency, poor stability of the iron-based catalyst system and the necessity of organic solvents are still serious limits for the application of [FeFe]–H_2ase mimics in large-scale H_2 production. The only two examples for H_2 generation in water catalyzed by [FeFe]–H_2ase models give rather low efficiencies with overpotentials larger than −0.9 V. Up to now, there have been no reports of electrocatalytic H_2 production by iron-based catalysts with water as a proton source, instead of acids. It is still a challenging and long-term task to learn the essential features of natural hydrogenases in their H_2 formation activity and uptake.

4.1.2 With cobalt complexes as the catalysts.

In 1980, Eisenberg and co-workers reported the first examples for electrocatalytic H_2 production by molecular catalysts in aqueous solutions.[26] Tetraazamacrocyclic cobalt complexes **35a** and **35b** (Fig. 9) could catalyze water reduction to H_2 at applied potentials of −1.6 and −1.5 V *vs.* SCE, respectively, with 80% Faradaic yield and 140–164 TON in bulk electrolysis experiments for 18 h (Table 7). In the following years, Grätzel and co-workers found that cobalt complexes **36** and **37** catalyzed the electrochemical reduction of water to H_2 in weakly acidic aqueous solutions at applied potentials of −0.7 V for **36** and −0.9 V *vs.* SCE for **37** (Table 7), giving 55% and 42% Faradaic yields, respectively.[32] A bulk electrolysis experiment using **38** as the catalyst in an aqueous solution at pH 5 with an applied potential of −1.15 V *vs.* SCE afforded 20 TON of H_2 evolution in 18 h.[33]

Very recently, Gray and co-workers reported that a cobalt bis(iminopyridine) complex **39** could act as a highly active electrocatalyst for water reduction to H_2 in an acidic aqueous solution with current densities >20 mA cm^{-2} at a pH-independent operating potential of −1.3 V *vs.* SCE.[77] Faradaic yields of ~75%, corresponding to 100 L h^{-1} (cm^2 Hg)$^{-1}$, were obtained from controlled potential bulk electrolysis performed at −1.4 V *vs.* SCE for 1 h in a buffered aqueous solution at pH 2 and ~87%, corresponding to 50 L h^{-1} (cm^2 Hg)$^{-1}$, at pH 5. The volume of H_2 evolved was greatly decreased at −1.0 V *vs.* SCE, regardless of the pH, indicating that **39** requires a relatively high overpotential

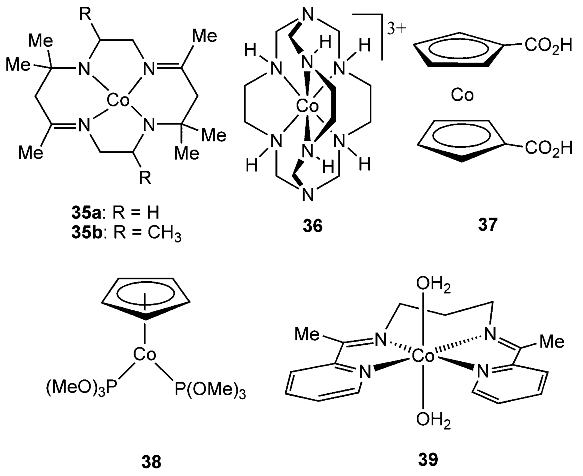

Fig. 9 The structures of cobalt complexes **35–39**.

Table 7 Electrocatalytic H_2 production by cobalt complexes *in acidic aqueous solutions*[a]

		Bulk electrolysis experiment				
Catalyst	OP[b] (V)	Medium	AP[c](V)	FY[d]	TON or TOF	Ref.
36	0.22	pH 4, KCl, phosphate buffer	−0.70	55%		32
37	0.28	pH 6.5, KCl, phosphate buffer	−0.90	42%		32
38	0.62	pH 5	−1.15		20 (18 h)	33
39	1.04	pH 2, NaP_i buffer	−1.40	~75%	100 L h^{-1} (cm^2 Hg)$^{-1}$	77
39	0.87	pH 5 citrate buffer	−1.40	~87%	50 L h^{-1} (cm^2 Hg)$^{-1}$	77

[a] Conditions: Hg pool or Hg drop electrode in H_2O. [b] OP = |applied potential *vs.* NHE − 0.059pH|. [c] AP = Applied potential *vs.* SCE. [d] FY = Faradaic yield.

to effectively reduce protons to H_2. A mechanism involving the initial reduction of the bis(iminopyridine) ligand and subsequent protonation has been proposed for this electrocatalytic H_2 generation reaction.

4.2 Electrocatalytic production of H_2 *in neutral aqueous solutions*

Although many earth-abundant metal complexes have been reported to be active for electrochemical H_2 generation, most of these complexes only catalyze proton reduction in organic solvents or mixtures of an organic solvent and water using inorganic or organic acids as proton sources at fairly negative potentials of −0.8 to −2.2 V. Only a few examples of earth-abundant metal molecular catalysts, which are able to electrochemically catalyze H_2 production from neutral aqueous solutions, have been reported in the literature.[28,78–80] The electrocatalytic results of H_2 production in neutral aqueous solutions with earth-abundant metal complexes as molecular catalysts are summarized in Table 8.

The molybdenum and cobalt pentapyridine complexes, $[(PY5Me_2)MoO]^{2+}$ (**40**) and $[(RPY5Me_2)Co(H_2O)]^{2+}$ (**41a**, Fig. 10) are the most efficient electrocatalysts ever reported for H_2 production in neutral aqueous solutions, with good stability but large overpotentials. Complex **40** catalyzes water reduction at −0.93 V (E_{on}) *vs.* NHE, corresponding to an overpotential of 0.52 V in phosphate buffer at pH 7 using a mercury pool electrode.[79] The electrocatalytic activity of **40** for water reduction on electrodes other than a mercury pool was not reported. A controlled potential electrolysis at −1.40 V *vs.* NHE in a phosphate buffer at pH 7 in a double-compartment cell gave a TON of 6.1×10^5 moles of H_2 per mole of catalyst with a TOF of 2.4 moles of H_2 per mole of catalyst per second with an overpotential of ~1.0 V. Catalyst **40** maintained catalytic activity under these conditions for at least 71 h. The catalytic water reduction stopped due to the high concentration of OH^- in the working electrode compartment. Furthermore, 1200 moles of H_2 per mole of catalyst per hour were obtained by controlled potential electrolysis experiments at −1.40 V *vs.* NHE in Californian sea water without an additional electrolyte. There are only another two nickel and cobalt molecular catalysts reported for electrochemical H_2 production in water at pH 7.[28,78] The efficiency of **40** is much higher than the previously reported nickel and cobalt catalysts **42–44** (Fig. 10). The controlled potential electrolysis experiment in neutral water with a mercury pool at −1.5 V *vs.* SCE for the macrocyclic dinickel(II) complex **42** gave TONs of H_2 evolution up to 100, with a TOF of 160 h^{-1} at an overpotential of 0.75 V and the experiment at −1.0 V *vs.* Ag/AgCl for the macrocyclic cobalt(III) hexaamine **43** afforded up to 5 TON, with a TOF of 0.4 h^{-1} at an overpotential of 0.39 V. Complex **44** displayed similar catalytic activity to **43**. Considering the catalytic activity and stability of the catalysts, the molybdenum-oxo-pentapyridine complex **40** is one of the most efficient molecular catalysts so far reported for H_2 production in neutral aqueous solutions without the requirement of any additional acids and/or organic cosolvents; however, the large overpotential needs to be reduced. A Mo^{II}/Mo^{IV} catalytic mechanism was proposed by Long and Chang for the generation of H_2 from water catalyzed by **40**, in which a $[(PY5Me_2)Mo(H_2O)]^{2+}$ intermediate was found to be responsible for the reductive cleavage of water to release H_2 and OH^- ions.[79]

Similar cobalt pentapyridine complexes (**41**, Fig. 10) are also robust and highly active catalysts for electrochemical production of H_2 from neutral water. The onsets of the catalytic currents occur at −1.00, −0.84 and −1.12 V *vs.* NHE, corresponding to overpotentials of 0.66, 0.43 and 0.71 V for $[(Py_5Me_2)Co(H_2O)](CF_3SO_3)_2$ (**41a**), $[(CF_3Py_5Me_2)Co(H_2O)](CF_3SO_3)_2$ (**41b**) and $[(Me_2NPy_5Me_2)Co(H_2O)](CF_3SO_3)_2$ (**41c**), respectively, in aqueous solutions maintained with phosphate buffer at pH 7, indicating that the reduction potential can be readily tuned by substitution on the pyridine ring.[80] A maximum TOF of 0.3 s^{-1} for **41a** was obtained by a 12 h bulk electrolysis experiment at −1.30 V *vs.* NHE in neutral water with 2.0 M phosphate buffer. No substantial loss in activity was observed over a 60 h bulk electrolysis experiment. As with molybdenum pentapyridine complex **40**, the catalytic activity of **41a** is terminated only by the high concentration of OH^- ions. The decomposition of the cobalt catalyst was not detected after 60 h of electrolysis.

5 Electrocatalytic H_2 production with earth-abundant metal complex-modified electrodes

5.1 A membrane electrode modified by nickel diazadiphosphine complexes

The technology to utilize the reduction of protons from water and the oxidation of H_2 in a regenerative fuel cell is very attractive because H_2 can be generated *in situ* when needed. Artero, Fontecave and Palacin together with their co-workers employed a nickel complex with DuBois' diazadiphosphine ligands in place of commonly used Pt catalysts in a fuel cell.[81] They prepared a membrane electrode assembly by first

Table 8 Electrocatalytic H_2 production by earth-abundant metal complexes *in neutral aqueous solutions*[a]

				Bulk electrolysis experiment				
Catalyst	Medium	E_{on} (V)[b]	OP[c] (V)	Medium	AP[d] (V)	TON	TOF (s^{-1})	Ref.
40	0.6 M phosphate buffer	−0.93	0.52	3.0 M phosphate buffer	−1.40	6.1×10^{-5} (71 h)	2.36	79
40	Californian sea water	−0.81	0.40	Californian sea water	−1.40		0.33	79
41a	1.0 M phosphate buffer	−1.07	0.66	1.0 M KCl	−1.40	FY ~ 100%		80
41a				2.0 M phosphate buffer	−1.30	5.5×10^{4} (60 h)	0.3 (12 h)	80
41b	1.0 M phosphate buffer	−0.84	0.43					80
41c	1.0 M phosphate buffer	−1.12	0.71					80
42	0.1 M $NaClO_4$, pH 7.4	−1.21	0.85	0.2 M phosphate buffer	−1.26	Up to 100	0.04	78
43				Phosphate buffer	−0.8	5 (12 h)		28

[a] Conditions: Hg pool, in H_2O, pH 7 unless otherwise noted. [b] E_{on} *vs.* NHE. [c] OP = overpotential = $|E_{on}$ *vs.* NHE − 0.059pH$|$. [d] Applied potential *vs.* NHE.

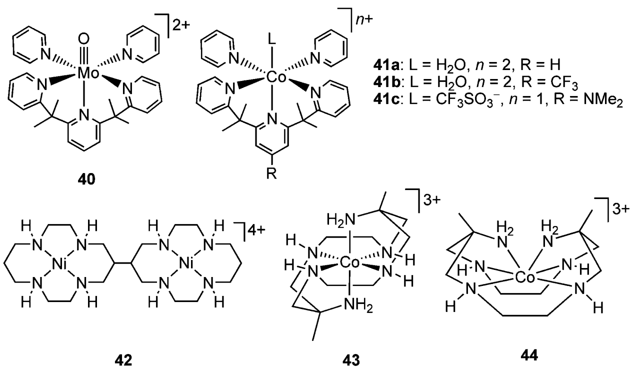

Fig. 10 The structures of the cobalt and molybdenum polypyridine complexes, as well as the macrocyclic dinickel(II) and cobalt(III) hexaamine complexes used as catalysts.

depositing multiwalled carbon nanotubes (MWCNTs) onto a Nafion membrane and then grafting the nickel catalyst to the MWCNTs (Fig. 11). This membrane electrode assembly displayed high electrocatalytic activity and exceptional stability under strongly acidic conditions. The current density was constant for more than 10 h at −0.3 V *vs.* NHE in 0.5 M H_2SO_4 (pH = 0–1), with more than 100 000 turnovers for H_2 evolution. The bioinspired nickel catalyst can reversibly catalyze the H^+/H_2 interconversion, functioning just like hydrogenases in nature. It is also very efficient for H_2 oxidation under the same conditions, with 35 000 turnovers of H_2 uptake during 10 h electrolysis at 0.3 V. Following this work, they adopted a straightforward methodology, namely, the π–π stacking functionalization of MWCNTs with pyrene-functionalized nickel complexes to prepare robust and bidirectionally electrocatalytic nanomaterials for H_2 evolution and uptake.[82] It has been demonstrated that most of the catalyst retains its molecular structure after grafting onto MWCNTs. The MWCMT-based nickel catalyst works bidirectionally, indicating an overpotential close to zero. These remarkable results, obtained by attaching the biomimetic nickel complexes to MWCNTs, show a new promising approach to economically viable regenerative fuel cells. These results show that the desired efficient and durable devices for electrochemical production and oxidation of H_2 in the presence of acids might be developed based on designed molecular catalysts composed of earth-abundant metals.

5.2 Electrodes modified by a cobaloxime complex

The mixture of complex **6a** was deposited together with black carbon on the surface of a glassy carbon (GC) electrode using a Nafion® 117 alcoholic solution.[83] Decomposition of a manganese molecular catalyst in Nafion has been found by Spiccia and co-workers.[84] Although the real structure of the catalyst after grafting is not known, this surface-modified GC electrode, referred to as GC|**6a** + BC|Nf (BC = black carbon, Nf = Nafion®), exhibits a response at E_{on} = −0.69 V *vs.* NHE in an aqueous H_2SO_4 (1 M) solution. The exchange current density for the GC|**6a** + BC|Nf electrode (~0.1 mA cm^{-2}) is 2 orders of magnitude higher than the GC electrode and 1 order of magnitude higher than the GC|BC|Nf electrode.

Complex **6a** was adsorbed on the surface of a GC electrode by controlled potential electrolysis at −0.6 V *vs.* SCE in the presence of TsOH in CH_3CN.[85] This chemically modified electrode is quite stable not only in CH_3CN but also in aqueous solutions. Although a low Faradaic yield (15%) was obtained from a homogeneous electrolysis experiment in phosphate buffer at pH 4, presumably due to the degradation of the catalyst **6a** during the electrolysis in the acidic aqueous solution, the GC electrode modified with **6a** displays significantly enhanced

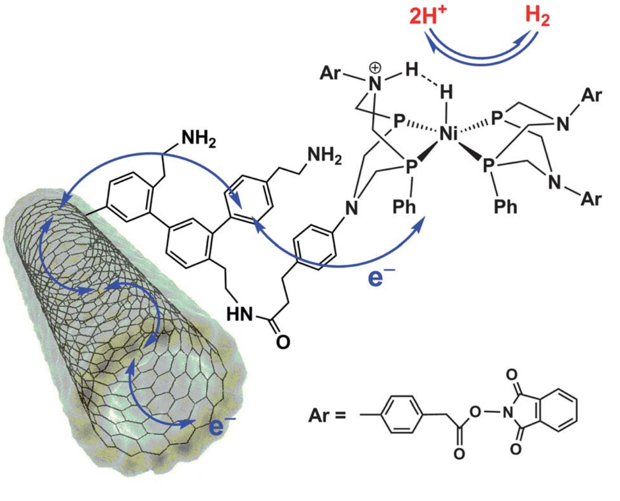

Fig. 11 A schematic representation of the structure of the bioinspired H_2-evolving nickel catalyst grafted on a carbon nanotube.[81]

catalytic activity and improved stability in aqueous solutions. The modified electrode is not catalytically active for H_2 generation in neutral water. However, at pH 2, the current increases by two orders of magnitude compared to the unmodified GC electrode, with the onset of the current increase occurring at −0.6 V *vs.* SCE (OP = 0.24 V). The controlled potential electrolysis (CPE) experiments at an applied potential of −0.90 V *vs.* SCE in an aqueous solution with phosphate buffer at pH 2 afford ~80% Faradaic yield and 5×10^5 TON (TOF ~ 20 s^{-1}) for H_2 production. The activity of the modified electrode remains constant for more than 7 h. Changing the phosphate buffer to an acetate buffer to achieve a pH of 4.5 in the aqueous solution results in the catalytic peak of the modified electrode appearing at −0.85 V *vs.* SCE, with the onset of the current increase occurring at −0.6 V *vs.* SCE (OP ~ 0.1 V). The bulk electrolysis experiments at an applied potential of −0.95 V *vs.* SCE in an aqueous solution with acetate buffer at pH 4.5 show a ~75% Faradaic yield and 5×10^6 TON for H_2 production in a 16 h electrolysis. Although the mechanism of the immobilization of complex **6a** on GC and the working principle of the modified electrode are still not clear, this electrode modified by cobaloxime complex **6a** features many advantages from an application point of view: 1) high activity with a relatively low overpotential, 2) greatly improved stability of the immobilized catalyst on the GC electrode as compare to that in homogeneous systems, 3) almost no leaching of the adsorbed catalyst from the GC electrode during a long period of electrolysis, 4) good performance in an acidic aqueous solution and without the requirement of any organic solvents.

5.3 Electrodes modified by diiron complex-functionalized electropolymer materials

Electrocatalytic H_2 production using electrodes modified by diiron mimics is scarcely reported. Pickett and co-workers covalently assembled a 2Fe3S complex to a poly(pyrrole) framework (Fig. 12), which was pre-electropolymerized on a glassy carbon or platinum electrode as a film (0.8–1 μm).[86] The non-functionalized polymer film electrodes are shown as GC|poly and Pt|poly and the diiron complex-functionalized ones are denoted as GC|$\text{poly}_{\text{FeFe}}$ and Pt|$\text{poly}_{\text{FeFe}}$. Electrocatalysis of proton reduction was studied on GC, GC|poly and GC|$\text{poly}_{\text{FeFe}}$ electrodes, respectively, under identical conditions. The catalytic peak for proton reduction appears at $E_{p/2} = -1.32$ V *vs.* Ag/AgCl on GC|poly in CH_3CN with 2,6-dimethylpyridinium cations (LuH^+) as the acid, which is *ca.* 90 mV more positive than that observed on the unmodified GC electrode. With GC|$\text{poly}_{\text{FeFe}}$ as the working electrode, the catalytic peak is further positively shifted to $E_{p/2} = -1.20$ V *vs.* Ag/AgCl. The current density at $E_{p/2}$ for proton reduction on GC|$\text{poly}_{\text{FeFe}}$ is about six times higher than on GC|poly at equivalent [LuH^+]. These results indicate that incorporation of diiron units of [FeFe]–H_2ase mimics in electropolymer films grown on an electrode can not only apparently enhance the efficiency but also reduce the overpotential of proton reduction.

6 Concluding remarks and outlook

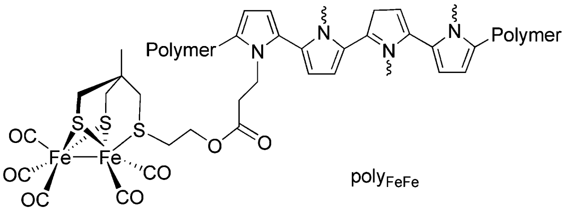

Fig. 12 The structure of the diiron complex-functionalized poly(pyrrole) material on GC and Pt electrodes.

Although encouraging progress has been achieved during the past years toward molecular catalyst systems free from noble metals for electrocatalytic H_2 production, there still exist many problems in the reported systems using organometallic complexes as catalysts. One of the crucial problems is that most molecular catalysts, including nickel complexes with base-containing diphosphine ligands, cobaloxime complexes and [NiFe]- and [FeFe]–H_2ase mimics, catalyze H_2 production only in organic solvents or mixtures of organic solvents with water with the requirement of extra acids as proton sources. The employment of organic solvents for the electrocatalytic reduction of water to H_2 will impede these molecular catalyst systems for future practical applications on a large scale. The other problems are low activities and large overpotentials for some molecular electrocatalysts regardless of the strength of the acids employed. Typical examples are the diiron complexes of the [FeFe]–H_2ase mimics. Although nearly one hundred synthetic diiron complexes have been synthesized and studied for electrocatalytic proton reduction to H_2, after the first report by Rauchfuss and co-workers in 2001,[54] most of them display low efficiencies and/or large overpotentials.[15] In general, cobaloxime complexes have small overpotentials, but they exhibit low catalytic rates of H_2 production.[9,10] Short-term durability under the conditions of H_2 evolution reactions is also a problem for most reported molecular electrocatalysts.

The molecular catalysts that can efficiently work in neutral aqueous solutions for electrochemical H_2 production are quite limited. Molybdenum and cobalt pentapyridine complexes **38** and **39** are unusual catalysts for electrochemical H_2 production as they work in neutral aqueous solutions. Novel catalysts based on earth-abundant metals with high efficiencies, small overpotentials and good durability for electrocatalytic H_2 production in neutral or near-neutral aqueous solutions are highly desired. In the future, with the smart design and synthesis of more earth-abundant metal-based molecular catalysts for electrochemical H_2 production without the requirement of extra acids and organic solvents, efficient cathodes built with cheap molecular catalysts for water reduction can be expected. In order to make a further step towards the construction of whole water-splitting photoelectrochemical cells by combination of the two half reactions of water oxidation and proton reduction, immobilization of molecular catalysts for hydrogen generation on the surfaces of cathode electrodes is a good way to proceed. More efforts focusing on this pathway are needed. Examination of the literature yields only limited approaches on the construction of photoelectrochemical devices for total water splitting. In 1998, Rocheleau and co-workers reported photoelectrochemical devices for hydrogen production using multijunction silicon photoelectrodes modified by CoMo hydrogen-evolving catalysts and $NiFe_yO_x$ oxygen-releasing catalysts.[87] A one-chip photovoltaic water electrolysis device using electrodes modified by similar catalysts was built by Ohmori and co-workers.[88] Very recently, Nocera and co-workers have reported a photoelectrochemical cell for total water splitting using modified electrodes with materials made from earth-abundant elements.[89] This pioneering work will encourage more researchers to pursue similar goals for purely electrocatalytic H_2 production or a combination of this with light-driven processes occurring directly in molecular devices.

Acknowledgements

We are grateful to the Natural Science Foundation of China (Grant No. 20633020 and 21120102036), the Basic Research Program of China (Grant No. 2009CB220009), the Swedish Energy Agency and the K & A Wallenberg Foundation for the financial support of this work.

References

1 M. Grätzel, *Acc. Chem. Res.*, 1981, **14**, 376–384.
2 A. J. Brad and M. A. Fox, *Acc. Chem. Res.*, 1995, **28**, 141–145.
3 R. Eisenberg and D. G. Nocera, *Inorg. Chem.*, 2005, **44**, 6799–6801.
4 N. Armaroli and V. Balzani, *Angew. Chem., Int. Ed.*, 2007, **46**, 52–66.
5 T. R. Cook, D. K. Dogutan, S. Y. Reece, Y. Surendranath, T. S. Teets and D. G. Nocera, *Chem. Rev.*, 2010, **110**, 6474–6502.
6 V. Artero and M. Fontecave, *Coord. Chem. Rev.*, 2005, **249**, 1518–1535.
7 J.-F. Capon, F. Gloaguen, P. Schollhammer and J. Talarmin, *Coord. Chem. Rev.*, 2005, **249**, 1664–1676.
8 J.-F. Capon, F. Gloaguen, F. Y. Pétillon, P. Schollhammer and J. Talarmin, *Coord. Chem. Rev.*, 2009, **253**, 1476–1494.
9 S. Losse, J. G. Vos and S. Rau, *Coord. Chem. Rev.*, 2010, **254**, 2492–2504.
10 V. Artero, M. Chavarot-Kerlidou and M. Fontecave, *Angew. Chem., Int. Ed.*, 2011, **50**, 7238–7266.
11 S. Canaguier, V. Artero and M. Fontecave, *Dalton Trans.*, 2008, 315–325.
12 M. R. DuBois and D. L. DuBois, *Acc. Chem. Res.*, 2009, **42**, 1974–1982.
13 D. L. DuBois and R. M. Bullock, *Eur. J. Inorg. Chem.*, 2011, 1017–1027.
14 V. V. Pavlishchuk and A. W. Addison, *Inorg. Chim. Acta*, 2000, **298**, 97–102.
15 G. A. N. Felton, C. A. Mebi, B. J. Petro, A. K. Vannucci, D. H. Evans, R. S. Glass and D. L. Lichtenberger, *J. Organomet. Chem.*, 2009, **694**, 2681–2699.
16 M. L. Helm, M. P. Stewart, R. M. Bullock, M. R. DuBois and D. L. DuBois, *Science*, 2011, **333**, 863–866.
17 G. A. N. Felton, R. S. Glass, D. L. Lichtenberger and D. H. Evans, *Inorg. Chem.*, 2006, **45**, 9181–9184.
18 V. Fourmond, P.-A. Jacques, M. Fontecave and V. Artero, *Inorg. Chem.*, 2010, **49**, 10338–10347.
19 C. J. Curtis, A. Miedaner, W. W. Ellis and D. L. DuBois, *J. Am. Chem. Soc.*, 2002, **124**, 1918–1925.
20 C. J. Curtis, A. Miedancer, R. Ciancanelli, W. W. Ellis, B. C. Noll, M. R. DuBois and D. L. DuBois, *Inorg. Chem.*, 2003, **42**, 216–227.
21 A. D. Wilson, R. H. Newell, M. J. McNevin, J. T. Muckerman, M. R. DuBois and D. L. DuBois, *J. Am. Chem. Soc.*, 2006, **128**, 358–366.
22 K. Fraze, A. D. Wilson, A. M. Appel, M. R. DuBois and D. L. DuBois, *Organometallics*, 2007, **26**, 3918–3924.
23 A. D. Wilson, R. K. Shoemaker, A. Miedaner, J. T. Muckerman, D. L. DuBois and M. R. DuBois, *Proc. Natl. Acad. Sci. U. S. A.*, 2007, **104**, 6951–6956.
24 U. J. Kilgore, J. A. S. Roberts, D. H. Pool, A. M. Appel, M. P. Stewart, M. R. DuBois, W. G. Dougherty, W. S. Kassel, R. M. Bullock and D. L. DuBois, *J. Am. Chem. Soc.*, 2011, **133**, 5861–5872.
25 M. R. DuBois and D. L. DuBois, *Chem. Soc. Rev.*, 2009, **38**, 62–72.
26 B. Fisher and R. Eisenberg, *J. Am. Chem. Soc.*, 1980, **102**, 7361–7363.
27 X. Hu, B. S. Brunschwig and J. C. Peters, *J. Am. Chem. Soc.*, 2007, **129**, 8988–8998.
28 P. V. Bernhardt and L. A. Jones, *Inorg. Chem.*, 1999, **38**, 5086–5090.
29 R. M. Kellett and T. G. Spiro, *Inorg. Chem.*, 1985, **24**, 2373–2377.
30 R. M. Kellett and T. G. Spiro, *Inorg. Chem.*, 1985, **24**, 2378–2382.
31 F. Zhao, J. Zhang, T. Abe, D. Wöhrle and M. Kaneko, *J. Mol. Catal. A: Chem.*, 1999, **145**, 245–256.
32 V. Houlding, T. Geiger, U. Kölle and M. Grätzel, *J. Chem. Soc., Chem. Commun.*, 1982, 681–683.
33 U. Koelle and S. Ohst, *Inorg. Chem.*, 1986, **25**, 2689–2694.
34 J. P. Bigi, T. E. Hanna, W. H. Harman, A. Chang and C. J. Chang, *Chem. Commun.*, 2010, **46**, 958–960.
35 G. M. Jacobsen, J. Y. Yang, B. Twamely, A. D. Wilson, R. M. Bullock, M. R. DuBois and D. L. DuBois, *Energy Environ. Sci.*, 2008, **1**, 167–174.
36 X. Hu, B. M. Cossairt, B. S. Brunschwig, N. S. Lewis and J. C. Peters, *Chem. Commun.*, 2005, 4723–4725.
37 C. Baffert, V. Artero and M. Fontecave, *Inorg. Chem.*, 2007, **46**, 1817–1824.
38 M. Razavet, V. Artero and M. Fontecave, *Inorg. Chem.*, 2005, **44**, 4786–4795.
39 P.-A. Jacques, V. Artero, J. Pécaut and M. Fontecave, *Proc. Natl. Acad. Sci. U. S. A.*, 2009, **106**, 20627–20632.
40 N. K. Szymczak, L. A. Berben and J. C. Peters, *Chem. Commun.*, 2009, 6729–6731.
41 O. Pantani, S. Naskar, R. Guillot, P. Millet, E. Anxolabéhère-Mallart and A. Aukauloo, *Angew. Chem., Int. Ed.*, 2008, **47**, 9948–9950.
42 W. R. McNamara, Z. Han, P. J. Alperin, W. W. Brennessel, P. L. Halland and R. Eisenberg, *J. Am. Chem. Soc.*, 2011, **133**, 15368–15371.
43 J. L. Dempsey, B. S. Brunschwig, J. R. Sinkler and H. B. Gray, *Acc. Chem. Res.*, 2009, **42**, 1995–2004.
44 C. H. Lee, D. K. Dogutan and D. G. Nocera, *J. Am. Chem. Soc.*, 2011, **133**, 8775–8777.
45 J. T. Muckerman and E. Fujita, *Chem. Commun.*, 2011, **47**, 12456–12458.
46 B. H. Solis and S. Hammes-Schiffer, *Inorg. Chem.*, 2011, **50**, 11252–11262.
47 M. Frey, *ChemBioChem*, 2002, **3**, 153–160.
48 V. Fourmond, S. Canaguier, B. Golly, M. Field, M. Fontecave and V. Artero, *Energy Environ. Sci.*, 2011, **4**, 2417–2427.
49 M. Wang, L. Chen, X. Li and L. Sun, *Dalton Trans.*, 2011, **40**, 12793–12800.
50 B. E. Barton, C. M. Whaley, T. B. Rauchfuss and D. L. Gray, *J. Am. Chem. Soc.*, 2009, **131**, 6942–6943.
51 B. E. Barton and T. B. Rauchfuss, *J. Am. Chem. Soc.*, 2010, **132**, 14877–14885.
52 S. Canaguier, M. Field, Y. Oudart, J. Pécaut, M. Fontecave and V. Artero, *Chem. Commun.*, 2010, **46**, 5876–5878.
53 V. Fourmond, S. Canaguier, B. Golly, M. J. Field, M. Fontecave and V. Artero, *Energy Environ. Sci.*, 2011, **4**, 2417–2427.
54 F. Gloaguen, J. D. Lawrence and T. B. Rauchfuss, *J. Am. Chem. Soc.*, 2001, **123**, 9476–9477.
55 S. Jiang, J. Liu, Y. Shi, Z. Wang, B. Åkermark and L. Sun, *Polyhedron*, 2007, **26**, 1499–1504.
56 L.-C. Song, J.-H. Ge, X.-F. Liu, L.-Q. Zhao and Q.-M. Hu, *J. Organomet. Chem.*, 2006, **691**, 5701–5709.
57 L.-C. Song, C.-G. Li, J. Gao, B.-S. Yin, X. Luo, X.-G. Zhang, H.-L. Bao and Q.-M. Hu, *Inorg. Chem.*, 2008, **47**, 4545–4553.
58 D. Chong, I. P. Georgakaki, R. Mejia-Rodriguez, J. Sanabria-Chinchilla, M. P. Soriaga and M. Y. Darensbourg, *Dalton Trans.*, 2003, 4158–4163.
59 R. Mejia-Rodriguez, D. Chong, J. H. Reibenspies, M. P. Soriaga and M. Y. Darensbourg, *J. Am. Chem. Soc.*, 2004, **126**, 12004–12014.
60 Y. Na, M. Wang, K. Jin, R. Zhang and L. Sun, *J. Organomet. Chem.*, 2006, **691**, 5045–5051.
61 P. Li, M. Wang, L. Chen, J.-H. Liu, Z.-B. Zhao and L. Sun, *Dalton Trans.*, 2009, 1919–1926.
62 L. Duan, M. Wang, P. Li, Y. Na, N. Wang and L. Sun, *Dalton Trans.*, 2007, 1277–1283.
63 L.-C. Song, Z.-Y. Yang, H.-Z. Bian, Y. Liu, H.-T. Wang, X.-F. Liu and Q.-M. Hu, *Organometallics*, 2005, **24**, 6126–6135.
64 L.-C. Song, J. Gao, H.-T. Wang, Y.-J. Hua, H.-T. Fan, X.-G. Zhang and Q.-M. Hu, *Organometallics*, 2006, **25**, 5724–5729.

65 L.-C. Song, J.-H. Ge, X.-G. Zhang, Y. Liu and Q.-M. Hu, *Eur. J. Inorg. Chem.*, 2006, 3204–3210.
66 J.-F. Capon, F. Gloaguen, P. Schollhammer and J. Talarmin, *J. Electroanal. Chem.*, 2004, **566**, 241–247.
67 J.-F. Capon, F. Gloaguen, P. Schollhammer and J. Talarmin, *J. Electroanal. Chem.*, 2006, **595**, 47–52.
68 G. A. N. Felton, A. K. Vannucci, J. Chen, L. T. Lockett, N. Okumura, B. J. Petro, U. I. Zakai, D. H. Evans, R. S. Glass and D. L. Lichtenberger, *J. Am. Chem. Soc.*, 2007, **129**, 12521–12530.
69 J. Chen, A. K. Vannucci, C. A. Mebi, N. Okumura, S. C. Borowski, M. Swenson, L. T. Lockett, D. H. Evans, R. S. Glass and D. L. Lichtenberger, *Organometallics*, 2010, **29**, 5330–5340.
70 F. Gloaguen, J. D. Lawrence, T. B. Rauchfuss, M. Bérard and M.-M. Rohmer, *Inorg. Chem.*, 2002, **41**, 6573–6582.
71 B. E. Barton, M. T. Olsen and T. B. Rauchfuss, *J. Am. Chem. Soc.*, 2008, **130**, 16834–16835.
72 Y. Na, M. Wang, J. Pan, P. Zhang, B. Åkermark and L. Sun, *Inorg. Chem.*, 2008, **47**, 2805–2810.
73 Z. Wang, J. Liu, C. He, S. Jiang, B. Åkermark and L. Sun, *Inorg. Chim. Acta*, 2007, **360**, 2411–2419.
74 P. Li, M. Wang, L. Chen, N. Wang, T. Zhang and L. Sun, *CrystEngComm*, 2008, **10**, 267–269.
75 C. M. Thomas, O. Rüdiger, T. Liu, C. E. Carson, M. B. Hall and M. Y. Darensbourg, *Organometallics*, 2007, **26**, 3976–3984.
76 M. L. Singleton, J. H. Reibenspies and M. Y. Darensbourg, *J. Am. Chem. Soc.*, 2010, **132**, 8870–8871.
77 B. D. Stubbert, J. C. Peters and H. B. Gray, *J. Am. Chem. Soc.*, 2011, **133**, 18070–18073.
78 J.-P. Collin, A. Jouaiti and J.-P. Sauvage, *Inorg. Chem.*, 1988, **27**, 1986–1990.
79 H. I. Karunadasa, C. J. Chang and J. R. Long, *Nature*, 2010, **464**, 1329–1333.
80 Y. Sun, J. P. Bigi, N. A. Piro, M. L. Tang, J. R. Long and C. J. Chang, *J. Am. Chem. Soc.*, 2011, **133**, 9212–9215.
81 A. L. Goff, V. Artero, B. Jousselme, P. D. Tran, N. Guillet, R. Métayé, A. Fihri, S. Palacin and M. Fontecave, *Science*, 2009, **326**, 1384–1387.
82 P. D. Tran, G. A. Le, J. Heidkamp, B. Jousselme, N. Guillet, S. Palacin, H. Dau, M. Fontecave and V. Artero, *Angew. Chem., Int. Ed.*, 2011, **50**, 1371–1374.
83 O. Pantani, E. Anxolabéhère-Mallart, A. Aukauloo and P. Millet, *Electrochem. Commun.*, 2007, **9**, 54–58.
84 R. K. Hocking1, R. Brimblecombe, L.-Y. Chang, A. Singh, M. H. Cheah, C. Glover, W. H. Casey and L. Spiccia, *Nature Chem.*, 2011, **3**, 461–466.
85 L. A. Berben and J. C. Peters, *Chem. Commun.*, 2010, **46**, 398–400.
86 S. K. Ibrahim, X. Liu, C. Tard and C. J. Pickett, *Chem. Commun.*, 2007, 1535–1537.
87 Richard E. Rocheleau, Eric L. Miller and Anupam Misra, *Energy Fuels*, 1998, **12**, 3–10.
88 Y. Yamada, N. Matsuki, T. Ohmori, H. Mametsuka, M. Kondob, A. Matsuda and E. Suzuki, *Int. J. Hydrogen Energy*, 2003, **28**, 1167–1169.
89 S. Y. Reece, J. A. Hamel, K. Sung, T. D. Jarvi, A. J. Esswein, J. J. H. Pijpers and D. G. Nocera, *Science*, 2011, **334**, 645–648.